

Hid, Rpr and Grim negatively regulate DIAP1 levels through distinct mechanisms

Soon Ji Yoo*§, Jun R. Huh*§, Israel Muro†, Hong Yu*, Lijuan Wang*, Susan L. Wang*, R. M. Renny Feldman*, Rollie J. Clem†, H.-Arno J. Müller‡¶ and Bruce A. Hay*#

*Division of Biology, MC156-29, California Institute of Technology, Pasadena, CA 91125, USA

†Molecular, Cellular and Developmental Biology program, Division of Biology, 232 Ackert Hall, Kansas State University, Manhattan, KS 66506, USA

‡Institut für Genetik, Heinrich-Heine Universität Düsseldorf, Universitätsstrasse 1, D-40225, Düsseldorf Germany

§These authors contributed equally to this work

e-mail: ¶muellera@uni-duesseldorf.de or #haybruce@its.caltech.edu



Published online: 14 May 2002; DOI: 10.1038/ncb793

Inhibitor of apoptosis (IAP) proteins suppress apoptosis and inhibit caspases. Several IAPs also function as ubiquitin-protein ligases. Regulators of IAP auto-ubiquitination, and thus IAP levels, have yet to be identified. Here we show that Head involution defective (Hid), Reaper (Rpr) and Grim downregulate *Drosophila melanogaster* IAP1 (DIAP) protein levels. Hid stimulates DIAP1 polyubiquitination and degradation. In contrast to Hid, Rpr and Grim can downregulate DIAP1 through mechanisms that do not require DIAP1 function as a ubiquitin-protein ligase. Observations with Grim suggest that one mechanism by which these proteins produce a relative decrease in DIAP1 levels is to promote a general suppression of protein translation. These observations define two mechanisms through which DIAP1 ubiquitination controls cell death: first, increased ubiquitination promotes degradation directly; second, a decrease in global protein synthesis results in a differential loss of short-lived proteins such as DIAP1. Because loss of DIAP1 is sufficient to promote caspase activation, these mechanisms should promote apoptosis.

Apoptosis is an evolutionarily conserved process through which organisms eliminate damaged or unwanted cells (reviewed in refs 1,2). Members of the caspase protease family are central components of the machinery that carries out this process^{3,4}. Most, if not all, cells express caspases sufficient to carry out apoptosis⁵. Because proteolysis is irreversible and caspases can amplify cascades of proteolysis, caspase activation and activity must be tightly regulated. The only known cellular caspase inhibitors are members of the IAP family^{6,7}. Many death-inhibiting IAPs have a carboxy-terminal RING domain. In many proteins, including several IAPs, this domain is necessary, and sometimes sufficient, to mediate E3 ubiquitin-protein ligase activity, catalysing the transfer of ubiquitin to E3-bound substrates⁸. This activity can promote auto-ubiquitination and subsequent IAP degradation, which presumably promotes apoptosis⁹. It can also promote the ubiquitination of bound caspases, presumably resulting in the inhibition of apoptosis^{10,11}. One important question is how IAP E3 activity is regulated. Evidence that such regulation is important comes from the observation in thymocytes that some death stimuli result in a decrease in IAP protein levels through a pathway that requires IAPs to be functional as E3s⁹. These observations suggest the existence of molecules that promote cell death by stimulating IAP ubiquitination. The *Drosophila* apoptosis inducer and IAP-interacting protein Hid is an interesting candidate because versions of DIAP1 that lack an intact RING domain are better able to protect against Hid-dependent death than wild-type versions^{12,13}.

In fact, we show here that expression of *Hid* results in a dramatic decrease in DIAP1 levels *in vivo*, and that this is associated with a corresponding increase in caspase activation. This activity requires DIAP1 ubiquitin-protein ligase activity, and *in vitro* assays demonstrate that Hid directly promotes DIAP1 ubiquitination and degradation. Expression of two other *Drosophila* apoptosis inducers,

Rpr and *Grim*, also result in the *in vivo* loss of DIAP1. Interestingly, this activity does not require the ubiquitin-protein ligase function of DIAP1, indicating that these proteins can regulate DIAP1 levels through a different mechanism. The *in vitro* observations with Grim described here, and with Rpr by Holley *et al.* (see note added in proof), show that these proteins can suppress general protein translation. Finally, we show that DIAP1 has a short half-life, whereas the half-life of the DIAP1-inhibitable apical caspase, Dronc, is much longer, and that loss of DIAP1 is sufficient to activate effector caspases. Together, these observations define two mechanisms through which IAP protein levels can be reduced in relation to the levels of apoptosis inducers.

Results

To characterize the relationship between IAP function and caspase activation *in vivo*, we generated an antibody that recognizes cleaved, and therefore active, versions of the effector caspase Drice¹⁴. This antibody specifically recognized dying cells. Labelling was present in many cells throughout the *Drosophila* wild-type stage 14 embryo (Fig. 1a), but was essentially absent from embryos homozygous for a chromosomal deletion (*H99*), which do not undergo normally occurring cell death¹⁵ (Fig. 1b). Anti-active Drice labelling (Fig. 1d) also correlated well with labelling of DNA fragmentation (Fig. 1c), which requires caspase activation in *Drosophila*^{16,17}.

DIAP1 functions in the early embryo to inhibit caspase activity. DIAP1 inhibits the activity of multiple *Drosophila* caspases^{18–21} and is required for the survival of many cells in the fly^{12,13,19,22}. Loss of DIAP1 in the embryo is associated with a large increase in DEVDase caspase activity, but in which cells caspase activation occurs is unknown¹⁹. We stained embryos that were homozygous for a loss-of-function allele of DIAP1, *th109*, with anti-active Drice

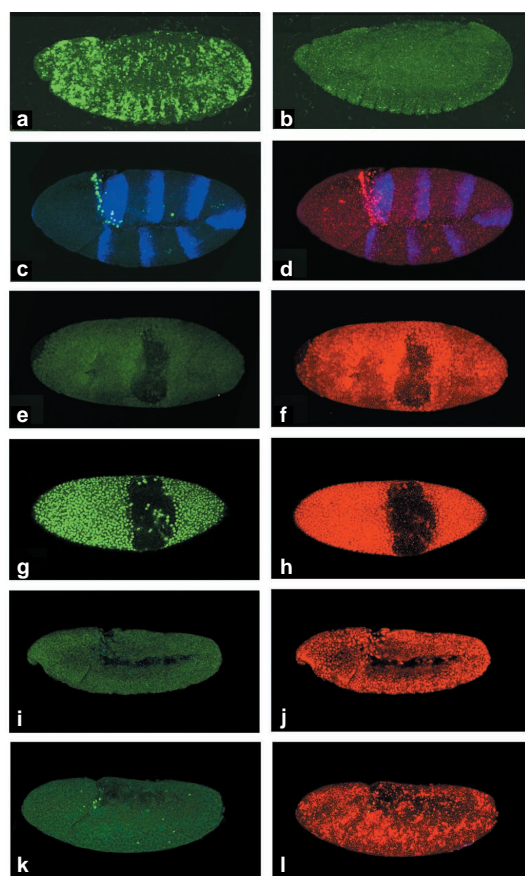


Figure 1 Loss of DIAP1 results in Drice activation. Confocal images of embryos of various genotypes are shown. **a**, The pattern of anti-active Drice-positive cells in a wild-type embryo (green). **b**, Active Drice-positive cells are absent from homozygous H99 embryos. **c**, The pattern of TUNEL-positive cells in a stage-10 embryo is shown (green). These embryos also express lacZ under the control of the *ftz* promoter. Anti- β -galactosidase staining is shown in blue. **d**, The embryo in **c** stained with anti-active Drice (red). **e**, A homozygous *th109* embryo at stage 8 stained for TUNEL (green). **f**, The embryo in **e** stained for active Drice (red). **g**, A *th109* embryo at stage 10 stained for TUNEL (green). **h**, The embryo in **g** stained for active Drice (red). **i**, TUNEL staining of a stage-10 embryo with genotype *mat67G4/mat67G4; mat15G4, th5/th5, UAS::p35*. This embryo is mutant for DIAP1, but survives because of *p35* expression. **j**, The embryo in **i** stained for *p35*. **k**, An embryo with the same genotype as **j** at stage 11 stained for TUNEL. **l**, The embryo in **j** stained with anti-active Drice. Anti-active Drice antibodies specifically recognize dying cells (**a,b**). Anti-active Drice labelling (**d**) shows good correspondence with TUNEL staining (**c**). Drice (**f**) becomes activated before TUNEL labelling appears (**e**). Ubiquitous expression of *p35* (**j**) rescues stage-10 (**i**) and -11 (**k**) embryos from cell death, as indicated by the essential lack of TUNEL labelling (green). However, ubiquitous expression of *p35* does not prevent the activation of Drice (**l**).

(refs 13,23). Essentially all cells contained activated Drice (Fig 1f,h). Initially, embryos could be identified that stained for active Drice (Fig. 1f), but lacked significant DNA fragmentation, as visualized with TUNEL staining (Fig 1e). Ultimately, however, cells became reactive to both probes (Fig. 1g,h). We also generated homozygous mutant *DIAP1* embryos, in which the baculovirus caspase inhibitor *p35* was ubiquitously expressed during early embryogenesis (Fig. 1j). In these embryos, Drice activation still occurred throughout the embryo at the extended germ-band stage (stage 10; Fig. 1l). However, through stage 11, DNA fragmentation was always largely absent (Fig. 1i,k). In addition, although embryos

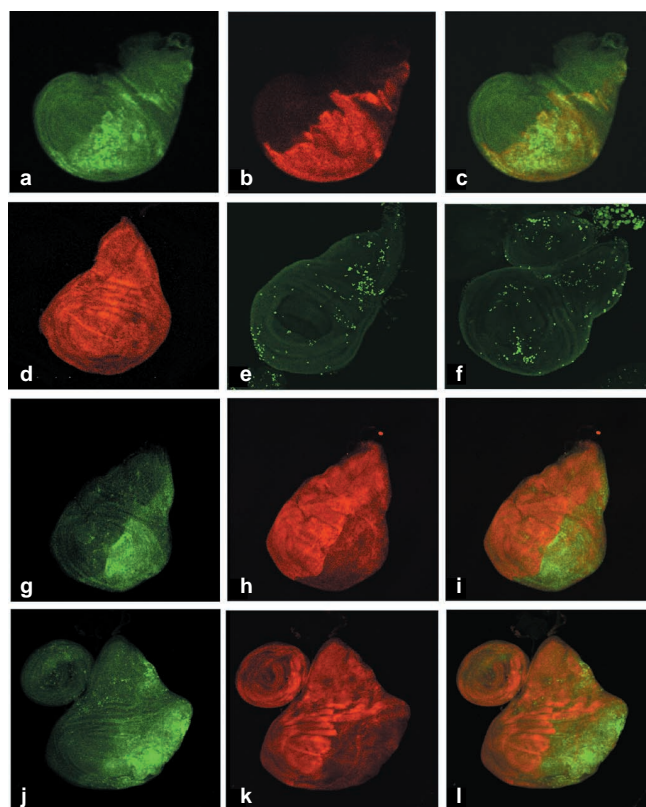


Figure 2 Expression of *Hid* or *Rpr* results in a loss of DIAP1 in *Drosophila* wing discs. Confocal images of wing discs from third-instar larvae of various genotypes. Posterior is to the right. **a**, Wing disc from a third instar larvae of genotype *UAS::Hid, UAS::p35; engrailed Gal4 (en::Gal4)*, stained with anti-*Hid* (green). **b**, Wing disc in a larvae stained with anti-*p35* (red). **c**, Merge of **a** and **b**. **d**, Wing disc of a larvae with genotype *UAS::p35; en::Gal4* stained with anti-DIAP1 (red). **e**, A *UAS::p35; enGal4* wing disc stained for TUNEL (green). **f**, A *UAS::Hid, UAS::p35; en::Gal4* wing disc stained for TUNEL (green). **g**, A *UAS::Hid, UAS::p35; en::Gal4* wing disc stained with anti-active Drice (green). **h**, The wing disc in **g** stained with anti-DIAP1 (red). **i**, merge of **g** and **h**. **j**, A wing disc of genotype *UAS::Rpr, UAS::p35; en::Gal4* stained with anti-active Drice (green). **k**, The wing disc in **j** stained with anti-DIAP1 (red). **l**, Merge of **j** and **k**. The *engrailed* promoter drives expression of *Hid* and *p35* in the posterior wing compartment (**a–c**). In the presence of *engrailed*-driven *p35*, *DIAP1* is expressed uniformly throughout the wing disc (**d**). Levels of TUNEL labelling in wing discs expressing *Hid* and *p35* (**f**) are similar to those of discs expressing *p35* alone (**e**). This, as well as the fact that *Hid*-expressing wing discs are morphologically normal, despite the fact that they have been expressing *Hid* for quite some time, argues that *p35* effectively suppresses *Hid*-dependent effector caspase activity. Expression of *Hid* under *engrailed* control results in Drice activation in the posterior wing compartment (**g**). This is associated with a corresponding decrease in DIAP1 in these same cells (**h,i**). Expression of *rpr* under control of the *engrailed* promoter also results in Drice activation in the posterior wing compartment (**j**). This is also associated with a corresponding decrease in DIAP1 levels (**k,l**).

homozygous for amorphic *DIAP1* alleles undergo morphogenetic arrest during germ-band extension (stage 8)¹⁹, *DIAP1* mutant embryos that expressed *p35* underwent normal morphogenesis until stage 11 (Fig. 1i,k). After this time, maternal *p35* was lost and massive cell death resumed (data not shown). Together, these observations make several points: first, loss of DIAP1 in the early embryo results in effector caspase activation in most, if not all, cells, and this activity is required for nuclease activation. Second, Drice activation is itself largely insensitive to the presence of *p35*. Third,

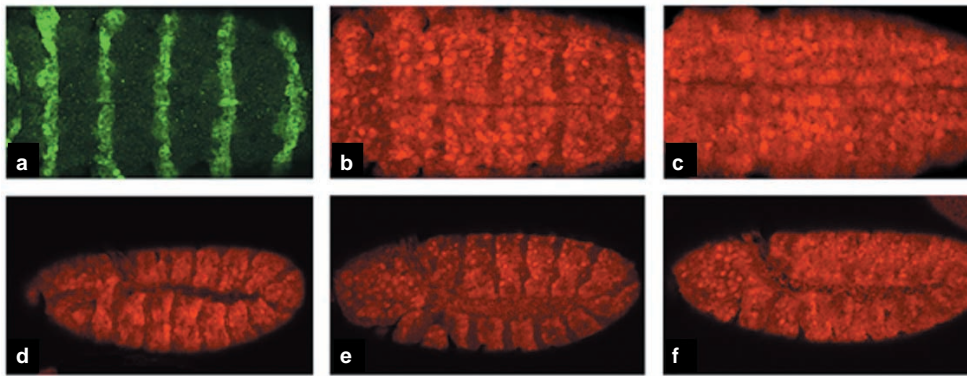


Figure 3 Expression of *Hid*, *Rpr* or *Grim* results in a loss of DIAP1 in the embryo. Confocal images of the ventral (a–c) or lateral (d–f) surfaces of embryos at stage 10 are shown. Anti-DIAP1 labelling is shown in red and anti-*Hid* labelling in green. **a**, An embryo with the genotype *UAS::Hid*, *UAS::p35*; *en::Gal4* stained with anti-*Hid* (green). **b**, The embryo in **a** stained with anti-DIAP1 (red). **c**, A wild-type embryo stained with anti-DIAP1 (red). **d**, A *UAS::Grim/en::Gal4*; *UAS::p35* embryo stained with anti-DIAP1 (red). **e**, A *UAS::Rpr/en::Gal4*; *UAS::p35* embryo stained

with anti-DIAP1 (red). **f**, An *en::Gal4*; *UAS::p35* embryo stained with anti-DIAP1 (red). DIAP1 expression is decreased in the *engrailed* expression domain, in which *Hid* is expressed (a–c). Embryos expressing *p35* under control of the *engrailed* promoter express DIAP1 ubiquitously (f). Embryos expressing *Grim* and *p35* (d), or *Rpr* and *p35* (e), under control of the *engrailed* promoter, show a large decrease in DIAP1 in the *engrailed* expression domain.

as Drice requires cleavage by other proteases for activation, loss of DIAP1 probably initially results in the activation of a p35-insensitive protease. Fourth, Dronc, a DIAP1-inhibitable, but p35-insensitive, caspase implicated in multiple death pathways, is a good candidate for such an activator^{20,21,24,25}. Consistent with this possibility, removal of Dronc in S2 cells through RNA interference prevented cell death induced by downregulation of DIAP1 (I.M. and R.J.C., manuscript submitted). Finally, the fact that *DIAP1* mutant embryos rescued from death by *p35* expression continued morphologically normal-looking development for several more hours is consistent with the hypothesis that the primary anti-apoptotic function of DIAP1, at least during early embryonic development, is to inhibit caspase activity.

***Hid*, *Rpr* and *Grim* downregulate DIAP1 *in vivo* through distinct, post-transcriptional mechanisms.** Because loss of DIAP1 is sufficient to promote cell-death-inducing caspase activity in many cells, it is important to understand how its activity is regulated. *Rpr*, *Hid* and *Grim* are essential apoptosis inducers in *Drosophila*²⁶. One mechanism through which they function involves binding to DIAP1, thereby directly suppressing its ability to inhibit caspase activity^{19,22,27}. A number of observations argue that these proteins also have other pro-apoptotic activities, but the relationship of these activities to the regulation of DIAP1 function is unknown^{22,28,29,30,31,32}. The control of IAP stability has recently emerged as an interesting possibility, based on the twin observations that IAPs can undergo auto-ubiquitination, thus promoting their own degradation, and that some death stimuli result in an increase in IAP ubiquitination⁹. Genetic evidence argues that *Hid* has a greater ability to promote apoptosis in the presence of wild-type DIAP1 than in the presence of RING mutated forms, consistent with the possibility that *Hid* promotes death by stimulating DIAP1 auto-ubiquitination and degradation^{12,13}. To examine this possibility directly, we characterized wing discs expressing *Hid* and *p35* in the posterior wing compartment, under the control of the *engrailed* promoter (Fig. 2a,b, respectively; Fig. 2c, merge). Co-expression of *Hid* and *p35* resulted in the activation of Drice in the posterior wing compartment (Fig. 2g). These cells showed a dramatic downregulation of DIAP1 levels (Fig. 2h,i). Importantly, this was not associated with an increase in Drice activity, as demonstrated by the fact that wing discs expressing *Hid* and *p35* showed low levels of DNA fragmentation (Fig. 2f), similar to those of wing discs expressing *p35* alone (Fig. 2e).

We also examined wing discs expressing *Rpr* and *p35* under control of the *engrailed* promoter. Drice became activated in the posterior wing compartment (Fig. 2j), and this was also associated with a dramatic loss of DIAP1 protein levels (Fig. 2k,l). Larvae expressing *Grim* and *p35* under the control of the *engrailed* promoter do not survive through late third-instar larval stages. Therefore we analysed the effects of *Grim* on DIAP1 levels in embryos. As in the wing disc, co-expression of *Hid* and *p35* under the control of the *engrailed* promoter resulted in a loss of DIAP1 in the cells that expressed *Hid* (Fig. 3 a,b; compare to 3c). Similar results were obtained when *Grim* or *Rpr* was co-expressed with *p35* (Fig. 3d,e, respectively). DIAP1 levels were dramatically lowered in a segmentally repeated pattern corresponding to the domain of *engrailed* expression. In both the wing disc and the embryo, expression of *Rpr* or *Grim* resulted in a greater decrease in DIAP1 levels than did expression of *Hid* (Figs 2,3). These differences may simply reflect differences in the strength of transgene expression. Alternatively, they may point towards differences in the mechanisms by which *Hid*, *Rpr* and *Grim* promote loss of DIAP1, or mechanisms by which their ability to mediate this loss is regulated.

To determine if expression of *Hid*, *Rpr*, or *Grim* was downregulating *DIAP1* transcript levels, we examined *DIAP1* expression levels in embryos of various genotypes. *DIAP1* was ubiquitously expressed in wild-type embryos, probably in all cells (data not shown). However, superimposed on this general pattern were domains in which levels of the *DIAP1* transcript were increased. These could be observed when *in situ* hybridizations were developed for a very short period of time (Fig. 4). At stage 10 (Fig. 4d), segmental modulation of DIAP1 is apparent. This repeated pattern overlaps with the parasegmental boundaries (Fig. 4f,h,j,l; arrows) and with the domains of *engrailed* expression (Fig. 4e,g,i,k). Importantly, levels of the *DIAP1* transcript within the *engrailed* domain, in which *Hid*, *Rpr* or *Grim* were expressed, were similar in wild-type (Fig. 4e,f), *Hid*-expressing (Fig. 4g,h), *Grim*-expressing (Fig. 4i,j) or *Rpr*-expressing (Fig. 4k,l) embryos. These observations do not rule out the possibility that *Hid*, *Rpr*, or *Grim* function as transcriptional regulators in some contexts. However, they do suggest that transcriptional downregulation of *DIAP1* is not a dominant mechanism to promote the loss of DIAP1 protein.

Together, these observations demonstrate that expression of *Hid*, *Rpr* or *Grim* results in a post-transcriptional loss of DIAP1. The *th6* mutant form of DIAP1 alters an essential cysteine residue

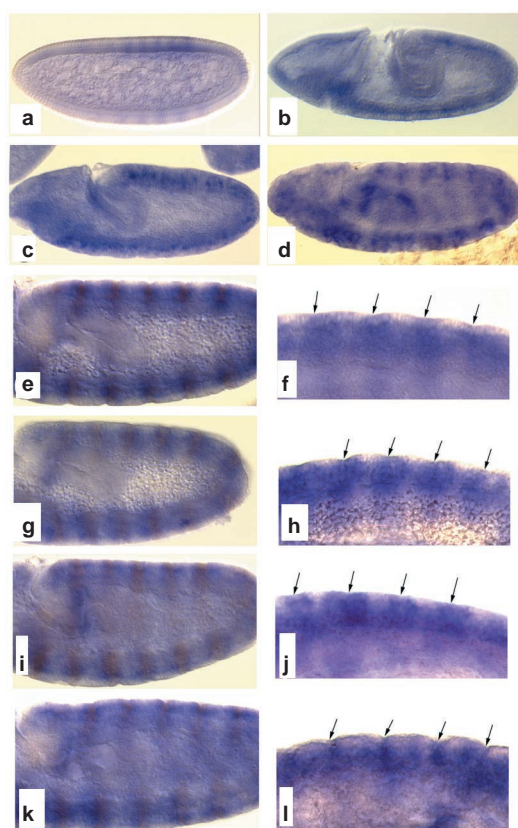


Figure 4 Expression of *Hid*, *Rpr* or *Grim* does not influence *DIAP1* transcript levels. Whole-mount *in situ* hybridizations of embryos of various genotypes with a digoxigenin-labelled *DIAP1* antisense mRNA, in blue (a–l). Anti-engrailed staining is shown in brown (e), as is anti-p35 staining (g,i,k). In wild type embryos, *DIAP1* is dynamically expressed during early development. *DIAP1* message is first detected in a uniform distribution in cleavage-stage embryos (data not shown). **a**, During cellularization (stage 5), *DIAP1* levels are increased in the dorsal blastoderm and in seven dorsoventral stripes. **b**, During gastrulation (stage 8), *DIAP1* is expressed at low uniform levels with moderately higher expression in the anterior mid-gut primordium, the posterior mid-gut and in neuroblasts. **c**, In the extended germ-band embryo (stage 9), high levels of *DIAP1* transcripts persist in the neuroblasts. Higher levels of transcript are also present in the proctodeum and anterior mid-gut. **d**, At stage 10, *DIAP1* shows prominent modulation of segmental expression. Stronger expression is now also seen in the proctodeum at the anlagen of the Malpighian tubules. The segmentally modulated expression of *DIAP1* observed in wild-type stage-10 embryos overlaps with the *engrailed* expression domain (immunolabelling with En antibodies seen in brown) (e), and with the position of the parasegmental grooves in stage-11 embryos (arrows in f). This pattern of *DIAP1* expression remains unimpaired in embryos expressing *Hid* (g,h), *Grim* (i,j) or *Rpr* (k,l) together with *p35* in the *engrailed* domain (immunolabelling with anti-p35 seen in brown). Embryos are shown as mid-sagittal optical sections at stage 10 (e,g,i,k) or as sagittal sections at stage 11 (f,h,j,l). The genotypes of the embryos are: **a–f**: wild-type. **g,h**: UAS::hid,UAS::p35; en::Gal4. **i,j**: UAS::grim /en::Gal4; UAS::p35. **k,l**: UAS::rpr/en::Gal4; UAS::p35.

in the *DIAP1* RING domain¹³ and results in a lack of E3 activity (Fig. 6b). To test whether the ability of *Hid*, *Rpr*, and *Grim* to reduce *DIAP1* levels requires *DIAP1* ubiquitin-protein ligase activity, we analysed the fate of the *th6* protein in tissues that expressed *p35* and one of these proteins. *th6* homozygotes die during embryogenesis. Wild-type *DIAP1* has a robust auto-ubiquitination activity and a short half-life of about 42 min (see Supplementary Information, Fig. S1). Thus, we reasoned that much of the *DIAP1*

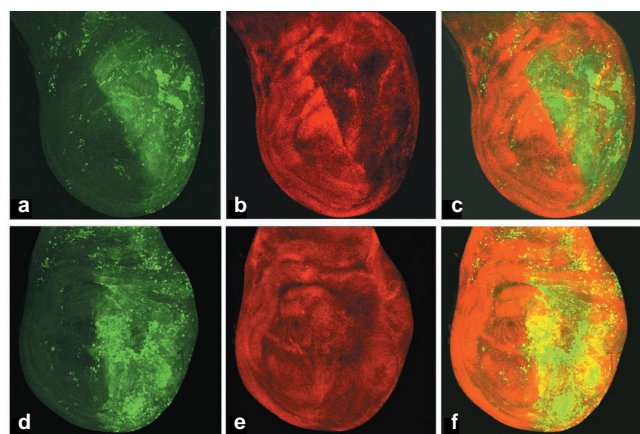


Figure 5 *Hid*-dependent downregulation of *DIAP1* requires *DIAP1* ubiquitin-protein ligase activity, but *Rpr*-dependent downregulation does not. Confocal images of wing discs of various genotypes stained with anti-active Drice and anti-*DIAP1*. Posterior is to the right. **a**, A wing disc of genotype UAS::Rpr/en::Gal4; UAS::p35/*th6* stained with anti-active Drice (green). **b**, A wing disc stained with anti-*DIAP1* (red). **c**, Merge of **a** and **b**. **d**, Wing disc of genotype UAS::Hid, UAS::p35; en::Gal4; *th6*/+ stained with anti-active Drice (green). **e**, Wing disc from **d** stained with anti-*DIAP1* (red). **f**, Merge of **d** and **e**. *Engrailed*-driven expression of *Rpr* and *p35* in *th6* heterozygote wing discs results in Drice activation and a corresponding decrease in *DIAP1* levels in the posterior wing compartment (a–c). *Engrailed*-driven expression of *Hid* and *p35* in *th6* heterozygote wing discs also results in Drice activation in the posterior wing compartment. However, *DIAP1* levels remain relatively constant throughout the wing disc (d–f).

protein present in *th6* heterozygotes was of the mutant form, as it lacked the ability of wild-type *DIAP1* to undergo auto-ubiquitination. Wing discs from *th6* heterozygotes that expressed *p35* and *Rpr* or *Hid* under the control of the *engrailed* promoter showed strong Drice activation in the posterior wing compartment (Fig. 5a,d). In the case of *Rpr*-expressing discs, this was associated with a strong decrease in *DIAP1* protein levels (Fig. 5b). In contrast, there was no appreciable difference in *DIAP1* levels between the anterior and posterior wing compartments in *Hid*-expressing wing discs from *th6* heterozygotes (Fig. 5e). Heterozygosity for *th6* did not appreciably diminish the ability of *Grim* to promote the disappearance of *DIAP1* in the embryo (data not shown). Based on these observations, we conclude that *Hid*, but not *Rpr* and *Grim*, promotes the loss of *DIAP1* through a mechanism that requires an intact RING domain.

***Hid* stimulates *DIAP1* polyubiquitination.** We introduced *DIAP1* into a ubiquitination assay containing E1, E2 (Ubc5) and ubiquitin, and characterized the *DIAP1* products by western blotting with an anti-*DIAP1* antibody. *DIAP1* was shifted into a ladder of high molecular weight species in a time-dependent manner (Fig. 6a). *DIAP1* was similarly upshifted in the presence of *Drosophila* embryo extract containing the proteasome inhibitor lactacystin (Fig. 6b). In contrast, *th6* *DIAP1* remained unchanged when incubated in the same system (Fig. 6b). Thus, *DIAP1* has E3 ubiquitin-protein ligase activity, resulting in auto-ubiquitination, and this requires an intact *DIAP1* RING domain. The failure of *th6* *DIAP1* to be modified in the presence of embryo extract is consistent with, but does not prove, that in this more complex system, the laddering seen with wild-type *DIAP1* was the result of auto-ubiquitination rather than ubiquitination by some other ligase. Addition of recombinant *Rpr* and *Grim* to this reaction did not result in an appreciable stimulation of *DIAP1* polyubiquitination (Fig. 6c). In contrast, addition of *Hid* resulted in a marked stimulation of

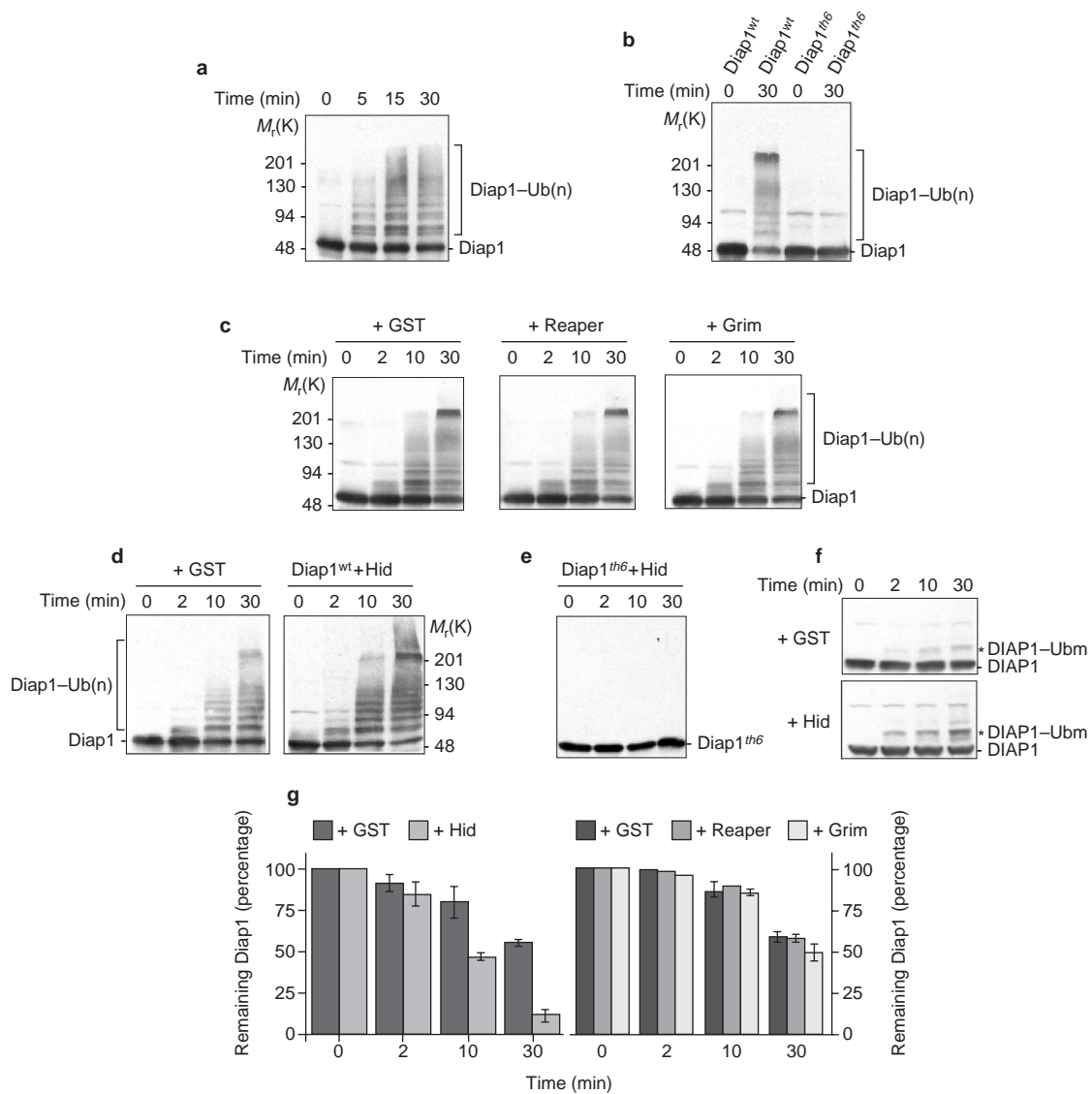


Figure 6 Hid stimulates DIAP1 polyubiquitination. Western blots are shown of wild-type DIAP1 and *th6* DIAP1 in combination with other factors, probed with an anti-DIAP1 antibody. **a**, DIAP1 underwent time-dependent polyubiquitination in a reaction consisting of purified E1, E2, DIAP1 and ubiquitin. Polyubiquitinated species of DIAP1 were upshifted, as indicated (Diap1-Ub(n)). **b**, Wild-type DIAP1 was also polyubiquitinated in *Drosophila* embryo extracts supplemented with the proteasome inhibitor lactacystin (compare 0 min with 30 min), but *th6* DIAP1 was not. **c**, DIAP1 underwent time-dependent polyubiquitination in the presence of embryo extract, lactacystin, and GST as a control. Substitution of Rpr or Grim for GST in this assay did not appreciably stimulate DIAP1 polyubiquitination further. **d**, In contrast, substitution of Hid for GST resulted in a strong stimulation of DIAP1 polyubiquitination, as indicated by the increased abundance of high molecular weight DIAP1-immunoreactive species at 10 and 30 min. **e**, Polyubiquitination of *th6* DIAP1 in

embryo extracts was not stimulated by Hid, nor was degradation of the unmodified DIAP1. **f**, DIAP1 underwent time-dependent mono-ubiquitination (DIAP1-Ubm) when embryo extracts containing GST were supplemented with methyl-ubiquitin. Substitution of Hid for GST in a similar reaction resulted in a stimulation of DIAP1 mono-ubiquitination. Hid did not stimulate a dramatic loss of unmodified DIAP1, arguing against the possibility that Hid stimulates the degradation of wild-type, unmodified DIAP1. **g**, Quantification of the time-dependent loss of unmodified DIAP1 in experiments similar to those shown in **c** and **d** for wild-type DIAP1. Time-zero was normalized to 100%. Hid promotes roughly a fivefold decrease in the levels of unmodified DIAP1 after 30 min of incubation (*n* = 5 independent experiments). Rpr and Grim did not appreciably stimulate loss of unmodified DIAP1 in comparison to assays that contained GST (*n* = 3 independent experiments).

DIAP1 polyubiquitination, as indicated by the increase in high molecular weight DIAP1 bands at 10 and 30 min (Fig. 6d). Importantly, however, though Hid bound *th6* DIAP1 as well as wild-type DIAP1 (Fig. 7c), it was unable to stimulate *th6* DIAP1 polyubiquitination (Fig. 6e). This suggests that Hid promotes DIAP1 auto-ubiquitination, rather than ubiquitination by some other E3. However, because *th6* DIAP1 is a mutant protein in which the RING structure has been disrupted, we cannot rule out the possibility that

it is simply unable to interact with a second E3 that mediates Hid-dependent stimulation of DIAP1 ubiquitination. However, the failure of *th6* DIAP1 levels to change in the presence of Hid argues against the possibility that the Hid-stimulated reduction of unmodified DIAP1 (Fig. 6c,d) occurs by activation a DIAP1-cleaving protease. This point is also suggested, but with wild-type DIAP1, by the results of ubiquitination assays containing wild-type DIAP1, glutathione S transferase (GST) and Hid in embryo extract,

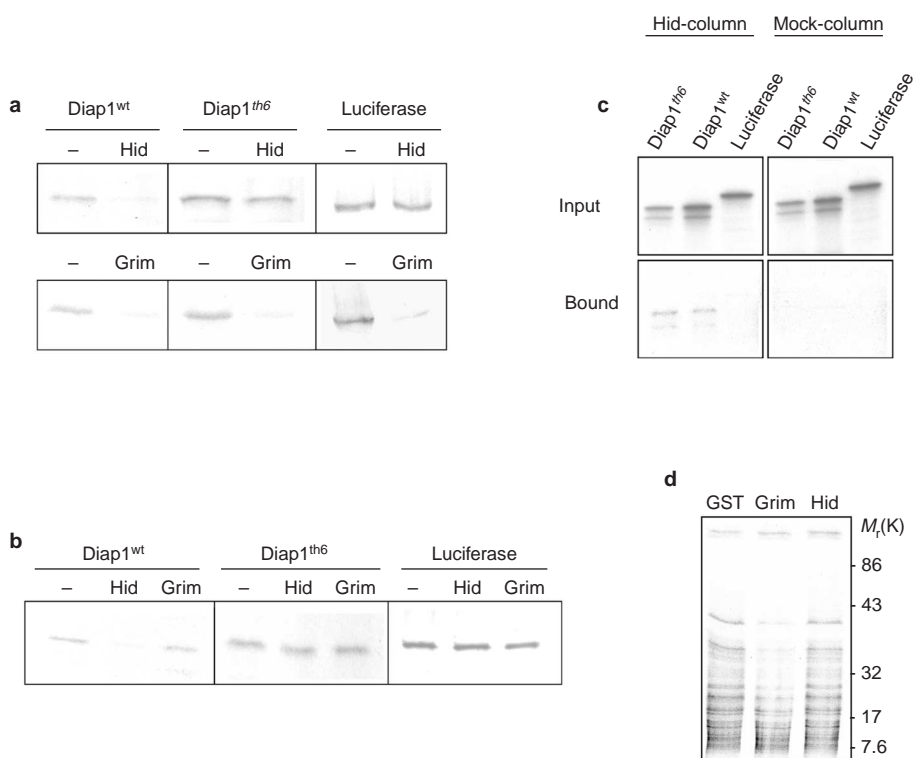


Figure 7 Hid induces a post-translational loss of DIAP1, whereas Grim causes a general suppression of translation. Wild-type DIAP1, *th6* DIAP1 or luciferase were translated in a reticulocyte lysate system in the presence of ³⁵S-methionine, either alone or in combination with Hid or Grim. Hid or Grim were also added to some reactions after translation termination. The products were visualized after SDS-PAGE. **a**, Hid suppressed the appearance of wild-type DIAP1 (DIAP1^{wt}), but not *th6* DIAP1 or luciferase, when added cotranslationally. In contrast, cotranslational addition of Grim resulted in a decrease in the appearance of all three proteins. **b**, Translation reactions for wild-type DIAP1, *th6* DIAP1 or luciferase were

either left untreated, or incubated with Hid or Grim. Post-translational addition of Hid resulted in a decrease in the levels of wild-type DIAP1, but not of *th6* DIAP1 or luciferase. Post-translational addition of Grim had no effect on the stability of any of the three proteins. **c**, *In vitro* translated versions of wild-type DIAP1, *th6* DIAP1 or luciferase were assayed for their ability to bind to Hid-bound beads. Wild-type DIAP1 and *th6* DIAP1 bound equally well to Hid beads, but did not bind to GST-beads. **d**, *Drosophila* translation extract supplemented with ³⁵S-methionine and either GST, Grim or Hid. Endogenous mRNAs drive the synthesis of multiple proteins. Grim, but not Hid, suppresses protein synthesis in this system.

in which methylated ubiquitin was added to the reaction. Methylated ubiquitin is unable to form polyubiquitin chains with substrate-bound ubiquitin³³. Thus, substrate proteins can only be mono-ubiquitinated, making it easier to analyse protein fate by SDS-polyacrylamide gel electrophoresis (PAGE). DIAP1 in the presence of embryo extract, GST, and methylated ubiquitin was mono-ubiquitinated in a time-dependent manner. As expected, substitution of Hid for GST stimulated DIAP1 mono-ubiquitination. However, it did not result in a large decrease in the levels of the unmodified form, which might suggest proteolytic cleavage (Fig. 6f). We observed a time-dependent loss of unmodified DIAP1 in all assays, reflecting its movement into higher molecular weight ubiquitinated forms (Fig. 6c,d,g). Hid, but not GST, Rpr or Grim, stimulated this loss greater than fivefold after 30 min of incubation (Fig. 6g).

Together, the above observations (as well as observations presented in Fig. 7) argue that Hid promotes DIAP1 ubiquitination, perhaps by stimulating auto-ubiquitination, and that this subsequently results in its degradation by the proteasome. Loss of DIAP1, as shown in the Fig. 1 for the DIAP1 mutant embryos, is sufficient to promote effector caspase activation. Thus, Hid combines two anti-DIAP1 pro-apoptotic functions: it directly inhibits the caspase-inhibiting activity of DIAP1 and promotes its degradation. Both of these activities should contribute to the observed increase in caspase activation in *Hid*-expressing cells (Figs 2, and 5).

Grim, but not Hid, can generally suppress translation. Rpr and Grim also promote the disappearance of DIAP1 *in vivo*. However, they did not appreciably stimulate DIAP1 polyubiquitination in a *Drosophila* extract. This lack of activity may reflect the adoption of unphysiological conformations by Rpr and Grim, or limitations of the assay used. For example, factors necessary for the ability of Rpr and Grim to stimulate DIAP1 ubiquitination might not be functional in the extract as prepared. This possibility is reflected by the observation that Hid did not significantly promote DIAP1 polyubiquitination in a purified reaction consisting of E1, E2, DIAP1 and ubiquitin, suggesting that other factors may be required (S.J.Y. and B.A.H., unpublished observations). Alternatively, Rpr and Grim might regulate a distinct step of ubiquitination stimulation that is not detected in our assay. For example, given the robust ubiquitination of DIAP1 in the embryo extract used, it is possible that proteins that stimulate ubiquitination by inhibiting inhibitors of ubiquitination would not be recognized as such. Notwithstanding these possibilities, several points can be made: Hid did function in the *Drosophila* embryo extract system. In addition, *in vivo* Rpr and Grim, but not Hid, promoted the loss of *th6* DIAP1, which is not functional as a ubiquitin ligase. Finally, although heterozygosity for *th6* resulted in a strong suppression of Hid-dependent cell death in the fly eye, consistent with a model in which Hid promotes apoptosis by stimulating DIAP1 degradation, heterozygosity for *th6* did not result in suppression of Rpr- or Grim-dependent cell death¹³. Together, these observations argue that Rpr and Grim are able to

regulate DIAP1 levels through post-transcriptional mechanisms distinct from those used by Hid. Inhibition of protein synthesis is often sufficient to induce apoptosis (see ref. 34 and references therein). To determine if Grim suppressed translation, we *in vitro* translated ³⁵S-labelled versions of wild-type DIAP1, *th6* DIAP1 or luciferase, alone or in the presence of recombinant Hid or Grim, in a rabbit reticulocyte system (Fig. 7a). The appearance of wild-type DIAP1 was largely eliminated by cotranslational addition of Hid (Fig. 7a), while the appearance of *th6* DIAP1 or luciferase was largely unaffected. In contrast, cotranslational incubation of translation reactions with Grim resulted in a large decrease in the appearance of all three proteins (Fig. 7a). Post-translational addition of Hid resulted in a decrease in the levels of wild-type DIAP1, but not of *th6* DIAP1 or luciferase, consistent with the idea that Hid promotes DIAP1 ubiquitination and degradation (Fig. 7b). Hid was, however, still able to bind *th6* DIAP1 (Fig. 7c). In contrast, post-translational addition of Grim had no effect on the abundance of wild-type DIAP1, *th6* DIAP1 or luciferase, suggesting that Grim was suppressing translation directly. We tested this hypothesis further in a *Drosophila* embryo extract translation system derived from 0–2-h-old embryos³⁵. Translation reactions were carried out in the presence of GST, Hid or Grim, and ³⁵S-labelled translation products derived from endogenous mRNAs were visualized after SDS-PAGE. In common with our observations in the reticulocyte lysate system, the presence of Grim, but not Hid, resulted in a significant decrease in total protein translation (Fig. 7d). The mechanism underlying this phenomenon is unlikely to involve caspase cleavage of translation factors³⁶, as Grim suppressed translation in reticulocyte lysates and *Drosophila* extracts in the presence of the potent caspase inhibitor zVAD. Finally, if Rpr and Grim promote apoptosis by inhibiting translation, then inhibition of protein synthesis in *Drosophila* might be expected to promote apoptosis. Consistent with this hypothesis, S2 cells exposed to cycloheximide died rapidly, adopting an apoptotic morphology (see Supplementary Information, Fig. S1).

These results, in conjunction with those of Holley *et al.* using Rpr (see note added in proof), argue that Grim and Rpr promote a general suppression of translation. Our experiments involved over-expression *in vivo* and the use of recombinant protein in extracts. Thus, we cannot rule out the possibility that Grim- and/or Rpr-dependent effects on translation reflect interactions with cellular components that would not normally occur. However, the hypothesis is imminently testable, as translational control targets can be identified. In addition, it will ultimately be important to demonstrate that endogenous levels of Rpr or Grim in identified cells fated to die, in the presence of caspase inhibitors, are sufficient to promote translational suppression, and that elimination of these genes results in a loss of translational suppression in these same cells.

Discussion

IAPs directly inhibit active caspases, and in addition, IAPs can promote their ubiquitination and degradation. Thus, IAPs constitute a last line of defence against death-inducing caspase activity. The importance of this function is made clear from our characterization of the DIAP1 loss-of-function phenotype. Loss of DIAP1 is sufficient to promote effector caspase activation in most, if not all, cells in the early embryo, and this activity is necessary for apoptotic nuclease activation. Thus, regulation of the relative levels of IAPs, and the caspases they inhibit, is one mechanism by which cells can control entry into apoptosis. Here, we describe two mechanisms through which DIAP1 ubiquitination regulates this balance. Hid stimulates DIAP1 ubiquitination and degradation directly. Grim (this work) and Rpr (see note added in proof) can promote a general suppression of protein translation. DIAP1 has a short half-life (about 40 min) because of its activity as a ubiquitin-protein ligase. But the half-life of an important target, the apical caspase Dronc, is much longer (about 3 h; see Supplementary Information Fig. S1).

Thus, all other things being equal, inhibition of protein synthesis will result in an imbalance in the relative levels of apoptosis inducers and inhibitors such as IAPs. In some cases, such as the early fly embryo, this alone will be sufficient to promote unrestrained caspase activation, whereas in other cases it may constitute a mechanism for sensitizing cells to other caspase-activating pathways. As mechanistic insight is gained into the workings of this pathway, it will be interesting to see if translational inhibition can be harnessed as a therapeutic tool. Finally, mutations that alter the RING domain stabilize IAPs (this work, refs 9,40). If these proteins retain the ability to inhibit caspases, they will function as better death inhibitors, thus inappropriately promoting cell survival. However, such mutated IAPs will also be unable to promote the ubiquitination and degradation of bound apoptosis inducers, such as caspases, and perhaps proteins such as Rpr, Hid, Grim or their mammalian counterparts, thus promoting cell death. Which outcome dominates is likely to be dependent on cell-type and the context. In either case, it will be interesting to see if C-terminal mutations in IAPs are associated with dysregulation of cell death in human disease.

Note added in proof: The work referred to as 'note added in proof' appears in this issue of Nature Cell Biology⁴⁰. Rpr promoted IAP ubiquitination in heterologous systems^{40,41}, but not in the early *Drosophila* embryo extracts utilized in this study. In addition, although Hid promoted the loss of DIAP1 in embryos and wing discs, and in *Drosophila* extracts (this work), it did not do so in eye imaginal discs⁴². These observations, coupled with the findings that DIAP1 ubiquitination is sensitive to the levels of two different E2s (refs 41–43), suggests that Rpr-, Hid- and Grim-dependent degradation of DIAP1 may be achieved through multiple pathways, and itself is likely subject to tissue-specific regulation. We also note that RING finger mutations may disrupt not only the auto-ubiquitination activity of IAPs, but also their ability to interact with other proteins that mediate ubiquitination in trans. Such differences may underlie the distinct behaviours of different RING mutant versions of DIAP1 (this work and ref. 41). In contrast to full-length Hid (this work), the failure of Hid^{1–37}-GST to promote DIAP1 ubiquitination⁴¹ is not surprising in the light of previous work demonstrating important apoptotic functions of the Hid C terminus⁴⁴. Finally, observed differences in the ability of Hid to promote the loss of DIAP1 *in vivo* (this work and ref. 41) can most simply be explained as being caused by differences in the strength of Hid transgene expression. □

Methods

Fly Strains

The following fly stocks were used: Oregon R. UAS::p35 (on third). UAS::p35 UAS::hid (onX). UAS::grim/UAS::grim (on2), UAS::p35/UAS::p35 (on3). UAS::rpr/UAS::rpr (on2); UAS::p35/UAS::p35 (on3). en::Gal4/en::Gal4 (ref. 37). *th109.07/TM3 [ftz::lacZ]*. *th5/TM3 [ftz::lacZ]*. *th6/TM3 [ftz::lacZ]*. *mat67G4/mat67G4*; *th5 mat15G4/Tm3 [ftz::lacZ]*. *th5 UAS::p35/TM3 [ftz::lacZ]*. en::Gal4 and *th6* were generous gifts from S. Crews and K. White, respectively. *mat67G4* and *mat15G4* are VP16-fusions with Gal4 driven by the maternal α -tubulin promoter (D. St Johnston and J.-P. Vincent, personal communication).

Antibody generation

Anti-active Drice-specific antibodies were raised in rabbits using a synthetic octapeptide, corresponding to residues surrounding the cleavage site of Drice (QRSQTETD) conjugated with Keyhole Limpet Haemocyanin (KLH) as the immunogen (Covance Research Products Incorporated, Richmond, CA). Active-Drice-specific antibodies were purified by sequential protein affinity purification methods. Antisera were first applied to a column bound with full-length inactive Drice (DriceC211A) to eliminate antibodies reactive to uncleaved Drice. The flow-through was applied to a Drice p21 subunit (residues 81–230) affinity column. Bound proteins were eluted using 100 mM glycine at pH 2.5. These antibodies detect the large fragment of active Drice, but do not recognize full-length Drice or the closely related caspase DCP-1 (J.R.H. and B.A.H., unpublished observations). Anti-Hid antibodies were produced in rabbits using full-length Hid with a C-terminal 6 \times His tag as the immunogen (Covance Research Products Inc). Anti-Dronc antibodies were produced in rabbits using a C-terminally 6 \times His-tagged version of the Dronc p20 subunit as the immunogen. An anti-DIAP1 monoclonal antibody was generated in mouse using a GST–DIAP1 fusion protein as the immunogen.

Fixation, immunolabelling and *in situ* hybridization of embryos

Embryos were collected and staged as described¹⁹. For immunolabelling, embryos were fixed with modified Stefanini's Fixative³⁸. For *in situ* hybridization, embryos were fixed with 8% paraformaldehyde in PBS. Immunolabelling and TUNEL assays were performed essentially as described¹⁹. *In situ*

hybridization with digoxigenin-labelled *DIAP1* antisense mRNA was performed subsequently³⁹. Antibodies were used at the following concentrations: rabbit anti-Drice (1:5000); rabbit anti-Hid (1:1000); mouse anti-p35 (1:10); mouse anti-DIAP1 (1:200); rabbit anti- β -Galactosidase (Cappel); 1:1500; mouse anti β -Galactosidase (1:1500; Promega, Madison, WI); mouse anti-Engrailed (1:10; DSHB, University of Iowa, Iowa City, IA). All secondary antibodies (Cy2-, Cy3-, Cy5- or horseradish peroxidase-conjugated) used were from Dianova (Jackson, West Grove, PA). The TUNEL kit was from Roche. Embryos or wing discs were mounted in Vectashield mounting medium (Vector, Burlingame, CA) and viewed with a Leica (Deerfield, IL) TCS-NT confocal microscope.

Preparation of recombinant *Drosophila* proteins

DIAP1-D20E was prepared as described previously³⁹ from GST-TEV-DIAP1-D20E before TEV cleavage. pET23a-Hid-6xHis and pET23a-Grim-6xHis were expressed in *Escherichia coli* BL21(DE3) pLys and purified under denaturing conditions. The pellet was dissolved in buffer S (6 M Guanidine-HCl, 100 mM NaH₂PO₄, 10 mM Tris-HCl at pH 8.0, 10 mM β -mercaptoethanol and 500 mM sodium chloride) before sonication and centrifugation. The supernatant was mixed with nickel-agarose (Qiagen, Valencia, CA) at room temperature for 1 h. The resin was washed with buffer WA (8 M urea, 100 mM NaH₂PO₄, 10 mM Tris-HCl at pH 8.0, 10 mM β -mercaptoethanol and 500 mM sodium chloride) four times and subsequently washed with buffer WB (buffer WA at pH 6.3). The protein was eluted with buffer EL (buffer WA at pH 4.5), and each protein was renatured by stepwise dialysis from 8–0 M urea buffer. Proteins were then dialysed into buffer UD (20 mM Tris-HCl at pH 7.5, 100 mM sodium chloride, 1 mM dithiothreitol (DTT) and 10% Glycerol). A full-length Rpr peptide was provided by S. Kornbluth and introduced into buffer UD before use.

Embryo extract preparation and ubiquitination assays

Drosophila embryo extract was made at 25 °C from 2–5-h-old embryos. Embryos were dechorionated with 50% bleach, rinsed, suspended in an equal volume of buffer EX (20 mM Tris-HCl at pH 7.5, 100 mM sodium chloride, 5 mM ATP, 2.5 mM magnesium chloride, 1 mM DTT and 0.25 M Sucrose) and homogenized. The supernatant was collected after centrifugation at 12,000g. The extract was adjusted to 10 μ g μ l⁻¹ with buffer EX. For ubiquitination assays with *Drosophila* embryo extract, GST, Hid, Rpr or Grim were pre-incubated with 1 μ l of embryo extract at room temperature for 20 min. Subsequently, DIAP1-D20E and His-ubiquitin (2 μ g total; Calbiochem, San Diego, CA) were added. The reaction was carried out in a final volume of 15 μ l of buffer UR (25 mM Tris-HCl at pH 7.5, 0.5 mM DTT, 2 mM ATP and 5 mM magnesium chloride). GST, Hid, Rpr or Grim were present at final concentrations of 1 μ M, and DIAP1 at 0.5 μ M. The reaction was carried out at 37 °C for various times. Reactions were stopped by addition of SDS sample buffer. DIAP1 was visualized using a mouse anti-DIAP1 antibody after SDS-PAGE and western blotting. NIH image software was used to quantify DIAP1-D20E band intensity. Ubiquitination reactions with purified proteins utilized E1 and E2 (GST-UbcH5A) purchased from Affiniti Research products (Nottingham, UK). DIAP1 (0.5 μ M, 400 ng) was incubated with 100 ng of E1 and 300 ng of E2, and 2 μ g of His-ubiquitin in buffer UR. Products were characterized as above.

In vitro translation reactions

Reticulocyte lysate translation reactions were carried out according to the manufacturer's instructions (Promega). Recombinant Hid and Grim were used at a final concentration of 7 nM and 70 nM, respectively. For cotranslational reactions, proteins were pre-incubated with reticulocyte lysate at 30 °C for 10 min before addition of RNA template. For post-translational assays, RNA templates were translated at 30 °C for 1 h. Reactions were terminated by a 5-min incubation with 0.8 μ g μ l⁻¹ RNase A (Qiagen), before addition of recombinant proteins. Translation products were resolved by 12% SDS-PAGE. *Drosophila* extract translation reactions were carried out as described previously³⁵, in the presence of recombinant GST, Hid or Grim (80 ng). Proteins were pre-incubated with embryo extract (provided by P. Zamore) at 25 °C for 10 min before addition of amino acid mix and ³⁵S-methionine. All translation reaction reactions included the general caspase inhibitor zVAD (100 μ M).

Hid binding assay

Reticulocyte-lysate-translated DIAP1, *th6* DIAP1 or luciferase were bound to 10 μ l of Affigel resin (Biorad, Hercules, CA) prebound with Hid or GST in binding buffer (25 mM HEPES at pH 7.5, 250 mM sodium chloride, 20 mM β -mercaptoethanol, 0.1% Triton-X100, containing the Complete EDTA-free protease inhibitor (Boehringer Mannheim, Indianapolis, IN). Samples were processed for SDS-PAGE analysis after multiple washes with binding buffer.

DIAP1 and Dronc half-life measurements and cell killing assay

6 \times 10⁶ S2 cells were seeded in TC-100 media containing 10% foetal bovine serum (Invitrogen, Carlsbad, CA) overnight. The next day, cycloheximide was added at 100 μ g ml⁻¹. Carrier (ethanol) was added alone to a separate well as a control. Cells were then harvested at 20-min intervals up to 140 min, centrifuged at 14,000g for 2 min before lysis in SDS-PAGE loading buffer. Lysate was run on SDS-PAGE gels and immunoblotted. Blots were analysed for DIAP1 using monoclonal anti-DIAP1, anti-mouse secondary antibody and SuperSignal chemiluminescent substrate (Pierce, Rockford, IL). Similarly, blots for Dronc were developed using rabbit anti-Dronc and the anti-rabbit secondary antibody. After measuring band intensity by densitometry, the results were tabulated and half-life was determined by best-fit analysis. To measure cell killing in response to cycloheximide, S2 cells were treated with 100 μ g ml⁻¹ cycloheximide or 0.1% ethanol as a carrier control. At 3, 6 and 12 h after treatment, viability was determined by comparing the number of intact cells to the number of intact cells at time-zero. Dying cells had typical apoptotic morphology.

RECEIVED 21 JANUARY 2002; REVISED 13 FEBRUARY 2002; ACCEPTED 11 MARCH 2002; PUBLISHED 14 MAY 2002.

1. Wyllie, A. H., Kerr, J. F. & Currie, A. R. Cell death: the significance of apoptosis. *Int. Rev. Cytol.* **68**, 251–306 (1980).
2. Raff, M. C. Social controls on cell survival and cell death. *Nature* **356**, 397–400 (1992).
3. Alnemri, E. S. *et al.* Human ICE/CED-3 protease nomenclature. *Cell* **87**, 171 (1996).

4. Thornberry, N. A. & Lazebnik, Y. Caspases: enemies within. *Science* **281**, 1312–1316 (1998).
5. Weil, M. *et al.* Constitutive expression of the machinery for programmed cell death. *J. Cell Biol.* **133**, 1053–1059 (1996).
6. Miller, L. K. An exegesis of IAPs: salvation and surprises from BIR motifs. *Trends Cell Biol.* **9**, 323–328 (1999).
7. Hay, B. A. Understanding IAP function and regulation: a view from *Drosophila*. *Cell Death Differ.* **7**, 1045–1056 (2000).
8. Pickart, C. M. Mechanisms underlying ubiquitination. *Annu. Rev. Biochem.* **70**, 503–533 (2001).
9. Yang, Y., Fang, S., Jensen, J. P., Weissman, A. M. & Ashwell, J. D. Ubiquitin protein ligase activity of IAPs and their degradation in proteasomes in response to apoptotic stimuli. *Science* **288**, 874–877 (2000).
10. Huang, H. *et al.* The inhibitor of apoptosis, clAP2, functions as a ubiquitin-protein ligase and promotes *in vitro* monoubiquitination of caspases 3 and 7. *J. Biol. Chem.* **275**, 26661–26664 (2000).
11. Suzuki, Y., Nakabayashi, Y. & Takahashi, R. Ubiquitin-protein ligase activity of X-linked inhibitor of apoptosis protein promotes proteasomal degradation of caspase-3 and enhances its anti-apoptotic effect in Fas-induced cell death. *Proc. Natl Acad. Sci. USA* **98**, 8662–8667 (2001).
12. Hay, B. A., Wassarman, D. A. & Rubin, G. M. *Drosophila* homologs of baculovirus inhibitor of apoptosis proteins function to block cell death. *Cell* **83**, 1253–1262 (1995).
13. Lisi, S., Mazzon, I. & White, K. Diverse domains of THREAD/DIAP1 are required to inhibit apoptosis induced by REAPER and HID in *Drosophila*. *Genetics* **154**, 669–678 (2000).
14. Fraser, A. G. & Evan, G. I. Identification of a *Drosophila* melanogaster ICE/CED-3-related protease, drICE. *EMBO J.* **16**, 2805–2813 (1997).
15. White, K. *et al.* Genetic control of programmed cell death in *Drosophila*. *Science* **264**, 677–683 (1994).
16. Hay, B. A., Wolff, T. & Rubin, G. M. Expression of baculovirus P35 prevents cell death in *Drosophila*. *Development* **120**, 2121–2129 (1994).
17. Yokoyama, H. *et al.* A novel activation mechanism of caspase-activated DNase from *Drosophila melanogaster*. *J. Biol. Chem.* **275**, 12978–12986 (2000).
18. Hawkins, C. J., Wang, S. L. & Hay, B. A. A cloning method to identify caspases and their regulators in yeast: identification of *Drosophila* IAP1 as an inhibitor of the *Drosophila* caspase DCP-1. *Proc. Natl Acad. Sci. USA* **96**, 2885–2890 (1999).
19. Wang, S. L., Hawkins, C. J., Yoo, S. J., Muller, H. A. & Hay, B. A. The *Drosophila* caspase inhibitor DIAP1 is essential for cell survival and is negatively regulated by HID. *Cell* **98**, 453–463 (1999).
20. Meier, P., Silke, J., Leever, S. J. & Evan, G. I. The *Drosophila* caspase DRONC is regulated by DIAP1. *EMBO J.* **19**, 598–611 (2000).
21. Hawkins, C. J. *et al.* The *Drosophila* caspase DRONC cleaves following glutamate or aspartate and is regulated by DIAP1, HID, and GRIM. *J. Biol. Chem.* **275**, 27084–27093 (2000).
22. Goyal, L., McCall, K., Agapite, J., Hartwig, E. & Steller, H. Induction of apoptosis by *Drosophila* reaper, hid and grim through inhibition of IAP function. *EMBO J.* **19**, 589–597 (2000).
23. Moore, L. A., Broihier, H. T., Van Doren, M., Lunsford, L. B. & Lehmann, R. Identification of genes controlling germ cell migration and embryonic gonad formation in *Drosophila*. *Development* **125**, 667–678 (1998).
24. Quinn, L. M. *et al.* An essential role for the caspase dronc in developmentally programmed cell death in *Drosophila*. *J. Biol. Chem.* **275**, 40416–40424 (2000).
25. Dorstyn, L., Colussi, P. A., Quinn, L. M., Richardson, H. & Kumar, S. DRONC, an ecdysone-inducible *Drosophila* caspase. *Proc. Natl Acad. Sci. USA* **96**, 4307–4312 (1999).
26. Vernooij, S. Y. *et al.* Cell death regulation in *Drosophila*: conservation of mechanism and unique insights. *J. Cell Biol.* **150**, F69–F76 (2000).
27. Wu, J. W., Cocina, A. E., Chai, J., Hay, B. A. & Shi, Y. Structural analysis of a functional DIAP1 fragment bound to grim and hid peptides. *Mol. Cell* **8**, 95–104 (2001).
28. Vucic, D., Kaiser, W. J. & Miller, L. K. Inhibitor of apoptosis proteins physically interact with and block apoptosis induced by *Drosophila* proteins HID and GRIM. *Mol. Cell Biol.* **18**, 3300–3309 (1998).
29. Wright, C. W. & Clem, R. J. Sequence requirements for hid binding and apoptosis regulation in the anti-apoptotic baculovirus inhibitor of apoptosis Op-IAP: Hid binds Op-IAP in a manner similar to Smac binding of XIAP. *J. Biol. Chem.* **277**, 2454–2462 (2002).
30. Chen, P., Lee, P., Otto, L. & Abrams, J. Apoptotic activity of REAPER is distinct from signaling by the tumor necrosis factor receptor 1 death domain. *J. Biol. Chem.* **271**, 25735–25737 (1996).
31. Wing, J. P., Zhou, L., Schwartz, L. M. & Nambu, J. R. Distinct cell killing properties of the *Drosophila* reaper, head involution defective, and grim genes. *Cell Death Differ.* **5**, 930–939 (1998).
32. Wing, J. P., Schwartz, L. M. & Nambu, J. R. The RHG motifs of *Drosophila* Reaper and Grim are important for their distinct cell death-inducing abilities. *Mech. Dev.* **102**, 193–203 (2001).
33. Hershko, A. & Heller, H. Occurrence of a polyubiquitin structure in ubiquitin-protein conjugates. *Biochem. Biophys. Res. Commun.* **128**, 1079–1086 (1985).
34. Fulda, S., Meyer, E. & Debatin, K. M. Metabolic inhibitors sensitize for CD95 (APO-1/Fas)-induced apoptosis by down-regulating Fas-associated death domain-like interleukin 1-converting enzyme inhibitory protein expression. *Cancer Res.* **60**, 3947–3956 (2000).
35. Tuschi, T., Zamore, P. D., Lehmann, R., Bartel, D. P. & Sharp, P. A. Targeted mRNA degradation by double-stranded RNA *in vitro*. *Genes Dev* **13**, 3191–3197 (1999).
36. Clemens, M. J., Bushell, M., Jeffrey, I. W., Pain, V. M. & Morley, S. J. Translation initiation factor modifications and the regulation of protein synthesis in apoptotic cells. *Cell Death Differ.* **7**, 603–615 (2000).
37. Han, K. & Manley, J. L. Functional domains of the *Drosophila* Engrailed protein. *EMBO J.* **12**, 2723–2733 (1993).
38. Muller, H. A. & Wieschaus, E. *armadillo*, *bazooka*, and *stardust* are critical for early stages in formation of the zonula adherens and maintenance of the polarized blastoderm epithelium in *Drosophila*. *J. Cell Biol.* **134**, 149–163 (1996).
39. Tautz, D. & Pfeifle, C. A non-radioactive *in situ* hybridization method for the localization of specific RNAs in *Drosophila* embryos reveals translational control of the segmentation gene hunchback. *Chromosoma* **98**, 81–85 (1989).
40. Holley, C. L., Olson, R. R., Colon-Ramos, D. A., & Kornbluth, S. Reaper-mediated elimination of IAP proteins through stimulated IAP degradation and generalized translational inhibition. *Nature Cell Biol.* DOI: 10.1038/ncb798.

- 41. Ryoo, H.D., Bergmann, A., Gonen, H., Ciechanover, A. & Steller, H. Regulation of *Drosophila* IAP1 degradation and apoptosis by *reaper* and *ubcd1*. *Nature Cell Biol.* DOI: 10.1038/ncb795.
- 42. Hays, R., Wickline, L. & Cagan, R. *Morgue* mediates apoptosis in the *Drosophila* retina by promoting degradation of DIAP1. *Nature Cell Biol.* DOI: 10.1038/ncb794.
- 43. Wing, J.P. *et al.* *Drosophila* Morgue is a novel F Box/ubiquitin conjugase domain protein important in grim-reaper mediated programmed cell death. *Nature Cell Biol.* DOI: 10.1038/ncb800.
- 44. Bergmann, A., Agapite, J., McCall, K. & Steller, H. The *Drosophila* gene *hid* is a direct molecular target of Ras-dependent survival signalling. *Cell* 95, 331–341 (1998).

ACKNOWLEDGEMENTS

We thank members of the Deshaies lab for their assistance with initial ubiquitination assays and S. Kornbluth for providing the Rpr peptide, and for sharing unpublished observations. We also thank

P.D. Zamore and members of his lab for providing the *Drosophila* embryo translation extract and translation protocols. We also thank G.M. Rubin and E. Kwan for the production of the anti-DIAP1 monoclonal antibody and K. White for *th6* flies. This work was supported in part by a grant from the Deutsche Forschungsgemeinschaft (MU1168/4-1) to H.-A.J.M. and grants from the Burroughs Wellcome Fund (New Investigator awards in the Pharmacological Sciences), the Ellison Medical Foundation, and a National Institutes of Health grant GM057422-01 to B.A.H. S.J.Y. was supported by a Jane Coffin Childs Postdoctoral fellowship.

Correspondence and requests for material should be addressed to H.-A.J.M. or B.A.H.

Supplementary information is available on *Nature Cell Biology's* website (<http://cellbio.nature.com>).

COMPETING FINANCIAL INTERESTS

The authors declare that they have no competing financial interests.

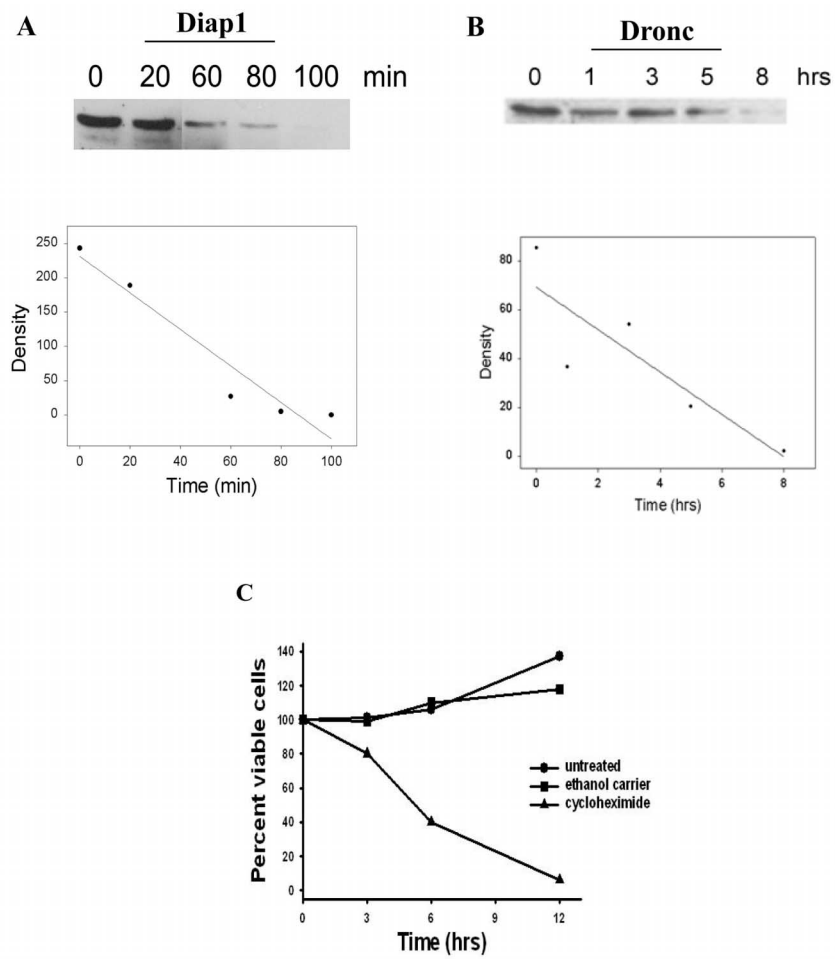


Figure S1 **DIAP1 and Dronc half-life in S2 cells.** The disappearance of DIAP1 and Dronc were monitored over time in S2 cells following Western blotting with

DIAP1- and Dronc-specific antibodies. **a**, DIAP1 has a half life of about 40 minutes. **b**, Dronc has a half life of about 3.1 hours. **c**, Cycloheximide kills S2 cells.